

Reliability modeling of mutual DCFP considering failure physical dependency

*

CHEN Ying, YANG Tianyu , and WANG Yanfang

Science and Technology on Reliability and Environmental Engineering Laboratory, Beihang University, Beijing 100191, China

Abstract: Degradation and overstress failures occur in many electronic systems in which the operation load and environmental conditions are complex. The dependency of them called dependent competing failure process (DCFP), has been widely studied. Electronic system may experience mutual effects of degradation and shocks, they are considered to be interdependent. Both the degradation and the shock processes will decrease the limit of system and cause cumulative effect. Finally, the competition of hard and soft failure will cause the system failure. Based on the failure mechanism accumulation theory, this paper constructs the shock-degradation acceleration and the threshold descent model, and a system reliability model established by using these two models. The mutually DCFP effect of electronic system interaction has been decomposed into physical correlation of failure, including acceleration, accumulation and competition. As a case, a reliability of electronic system in aeronautical system has been analyzed with the proposed method. The method proposed is based on failure physical evaluation, and could provide important reference for quantitative evaluation and design improvement of the newly designed system in case of data deficiency.

Keywords: electronic system, dependent competing failure process (DCFP), failure physical dependency, threshold descent model, competition failure modes.

DOI: [10.23919/JSEE.2023.000108](https://doi.org/10.23919/JSEE.2023.000108)

1. Introduction

Due to the complexity of structures and the environment, electronic system may undergo different types of failure. The failures can be divided into two categories from the aspect of the failure mechanism, namely degradation failure and shock (or overstress) failure; they are also respectively called soft failure and hard failure. In recent years, the dependent competing failure process (DCFP) has been widely investigated by researchers, involving two

failure processes, one is soft failure caused by continuous degradation together with additional abrupt degradation due to a shock process, the other is hard failure caused by the instantaneous stress during the same shock process. It is very important to understand and describe the failure mechanisms of DCFP for predicting reliability and making reasonable testing strategies.

Recently, the failure dependency of the DCFP, which includes both unilateral and mutual dependence, has drawn the attention of researchers. Unilateral dependence means that in the system, shock process and degradation process only have one-sided influence, for example, only shock on the degradation process, or only degradation on the shock process, and there is no coupling between them.

Many researches have been focused on unilateral dependencies, which includes the shock-degradation dependencies and the degradation-shock dependencies. The former indicates that the shock process may increase the degradation level or degradation rate. Wang et al. [1,2] believed that nonfatal shocks would increase the degradation level and degradation rate by a specific cumulative shock amount. Hao et al. [3] and Kong et al. [4] believed that shocks may affect the degradation rate, as well as the hard failure threshold level. Gao et al. [5] considered the dependency between the soft and hard failure processes in terms of two different system effected processes (SEPs), namely the degradation level and degradation rate. Shen et al. [6] studied the reliability of a multicomponent system subject to DCFP, where the shocks process may cause sudden jump in the degradation level or accelerating the degradation rate. Fan et al. [7] supposed that dependence arises due to the abrupt changes to the degradation processes brought by random shocks. Tang et al. [8] developed reliability models for DCFP systems, considering the correlation between additional damage size on degradation in soft failure process and

Manuscript received February 03, 2021.

*Corresponding author.

This work was supported by the National Natural Science Foundation of China (61503014; 62073009).

stress magnitude of shock load in hard failure process.

Also, many studies have been devoted to the degradation-shock effect. Ye et al. [9] developed a shock model in which shocks arrive according to a nonhomogeneous Poisson process (NHPP) and the destructive probability depends on the remaining hazard of the degradation. Fan et al. [10] assumed that the intensity of a random shock process was dependent on the degradation process. Zhu et al. [11] indicated that the system was subject to competing wear and shock failures, and that the threshold relied on the deterioration level. Rafiee et al. [12] believed that the hard failure threshold may change with the degradation process, and studied two cases. Many other studies assumed that the hard failure threshold may not be only affected by the degradation process [11,13–15], but also by itself. Systems have been found to continue deteriorating with the continued reduction of failure resistance while under the pressure of shocks and degradation [16–19].

The shock and degradation processes of DCFP also have mutual dependency. Some studies considered an abrupt increase caused by shocks on the degradation performance and the decrease of the threshold level due to the degradation process [20–22]. Some assumed that shocks could accelerate the degradation process by causing sudden degradation increments, and that degradation would impact shock intensity [23].

Previous research has made various significant contributions to the challenging problem of DCFP reliability evaluation. Very few publications studied the mutual dependency. Furthermore, failure mechanism of electronic products and their correlation have become the research hot spot and a great deal of progress has been made to understand the DCFP and other degradation effect [24–27]. Chen et al. proposed many types of failure mechanism dependencies, including acceleration, inhibit, trigger and parameter union [28–30]. However, the mutual DCFP of electronic system has not been widely recognized and modeled.

In this paper, the DCFP effect in electronic system is studied and modeled from the aspect of failure physical dependency, which includes acceleration, accumulation, and competition of failure mechanisms. Researchers have shown that avionics system may have two types of failure mechanisms due to fatigue and electromagnetic interference, namely the degradation failure of thermal fatigue and/or vibration fatigue, and overstress failure caused by intermittent electrical shocks. The mutual dependency is decomposed into the interaction between failure mechanisms. The reliability model is constructed and the degradation is considered as stochastic process.

The contributions of this paper can be summarized as follows. Firstly, a shock-degradation acceleration model is presented to describe the acceleration effect of the shock process on degradation based on the dependence of failure mechanisms. Secondly, a threshold descent model is constructed to describe the cumulative effect of both types of failures on the hard failure threshold. Finally, the dynamic reliability of the electronic system is evaluated considering the mutual DCFP effect, which provides the reliability modeling method for this kind of coupling problem.

The remainder of this paper is organized as follows. Section 1 summarizes the current research status of failure dependency in DCFP. Section 2 describes the background and mutual dependence effect. Section 3 presents the shock-degradation acceleration model and the threshold descent model. Section 4 presents a case study of electronic system in an avionics system. The dynamic reliability of the system with a mutually dependent competing failure process is evaluated. Finally, Section 5 summarizes the conclusions of this paper and outlines the directions for future research.

2. Background and assumption

Electronic systems are designed to be more and more complicated and resistant to failure. The physics-of-failure (PoF) method is widely used to study the failure mechanism and the reliability of the components. The characteristic of this method is to establish the degradation or lifetime equations while considering parameter uncertainties. However, failure mechanisms are usually used to describe the microlevel behavior, and the dependency between failure mechanisms is of great importance for modeling of complex electronic systems.

The mutual dependencies of the DCFP in electronic system are presented in Fig. 1. Two main failure processes are considered here, namely soft failure caused by the continual degradation process and hard failure caused by the stress from the random shock process. Continuous degradation is a process of fatigue crack initiation and propagation, it can be modeled with PoF equations. The Coffin-Manson model serves as an appropriate model for thermal fatigue, and has been mentioned in many existing works. Electrical shock will not cause an open circuit at the initial stage of operation, which means that although the damage due to electrical shock will not reach the threshold of hard failure, it will induce the deterioration of material performance, and fatigue cracks will develop more rapidly. Shocks will increase the degradation rate (acceleration effect), and the amount of degradation has an abrupt decrease in the degradation level when

one shock arrives. Moreover, the material deterioration caused by electrical shock (shock process) and fatigue

crack growth (degradation process) will decrease the threshold of open circuit failure.

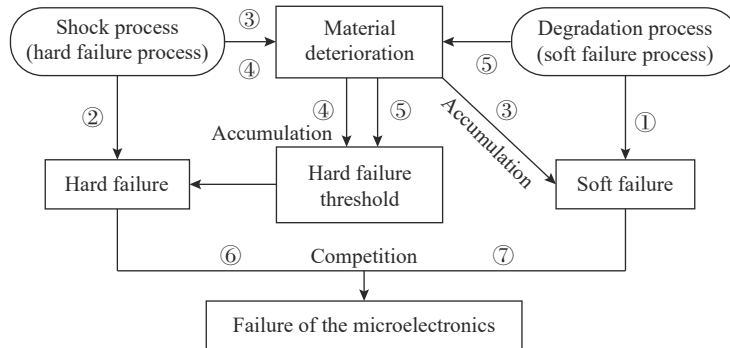


Fig. 1 Dependencies DCFP in electronic system

The electronic system is subject to the mutual dependence between degradation and random shocks. As described in Fig. 1, line ① indicates the degradation process due to environmental or operating loads. Line ② refers to hard failure due to the shock process. When the shock process exceeds the hard failure threshold, hard failure will occur. Line ③ is the shock degradation dependence process, whereby the arriving shocks accelerate the degradation process by increasing the degradation rate and the amount of degradation. In addition, considering the degradation-shock dependence, lines ④ and ⑤ indicate that the hard failure threshold will decrease because of the degradation and shock process. In addition, they have a cumulative effect, which can be expressed by linear or nonlinear cumulative rules. Finally, the failure is determined by the completion of lines ⑥ and ⑦.

Failure mechanism tree (FMT) is used to model the correlations of failure mechanisms, which was proposed by Chen et al. [28]. The FMT of Fig. 1 can be constructed and shown in Fig. 2.

represents the impact of the degradation failure mechanism on the hard failure threshold, and there is a cumulative relationship between them. Additionally, M_D represents the degradation process, M_S represents the shock process, and M'_D represents the degradation process after accelerated by M_D and M_S . ‘ Δ ’ indicates that this is a trigger event, and S, H, and F represent soft failure, hard failure, and component failure, respectively. Finally, “MACC”, “MADA”, and “MACO” represent the failure physical dependencies of acceleration, accumulation, and competition, respectively.

Based on the preceding description, the following assumptions are required:

- (i) The electronic system is non-repairable, and the failure mechanisms are all in binary state.
- (ii) The electronic system consists of one hard failure and one degradation failure. The shock arrival time follows homogeneous Poisson process, and the shock intensity is normally distributed.
- (iii) The decrease of the hard failure threshold is linearly related to the material deterioration caused by the degradation and shock processes.

3. Acceleration and threshold descent model

3.1 Shock-degradation acceleration model

As mentioned previously, the degradation process will be accelerated by the shock process which is illustrated in Fig. 3, where w_i is the shock load spectrum and $X(t)$ is the damage of the degradation process. Each time that shock arrives (the time interval is $T_i(i = 1, 2, \dots, n)$), the shock will increase the degradation rate and cause sudden increase on degradation as $d_i(i = 1, 2, \dots, n)$. Additionally, H_0 is the limit of soft failure, and $w_i(i = 1, 2, \dots, n)$ are the load of individual shocks, $W(t)$ is the load at time t and D_0 is the initial hard failure threshold. Hard failure will occur when w_i exceeds the hard failure threshold, which will be described in detail in Subsection 3.2.

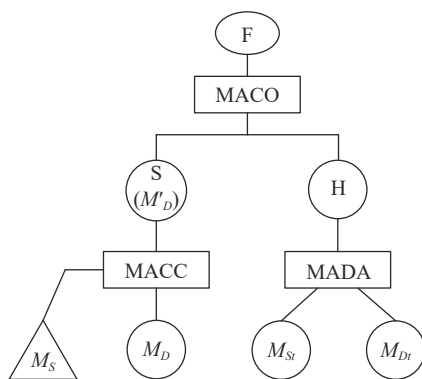


Fig. 2 Failure mechanism tree of Fig.1

In Fig. 2, M_{S_r} represents the impact of the shock failure mechanism on the hard failure threshold and M_{D_r} rep-

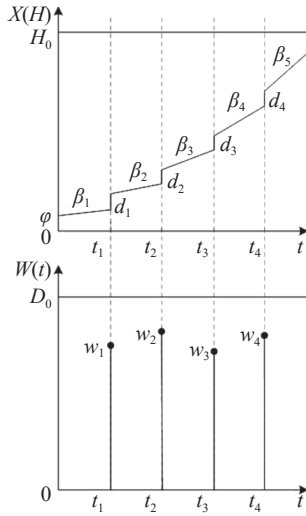


Fig. 3 Shocks affecting degradation rate

In Fig. 3, the soft failure occurs when degradation exceeds the degradation limit H_0 . The total degradation of $X(t)$ can be expressed as

$$X(t) = \varphi + Y(t) + S(t) \quad (1)$$

where φ is the initial degradation level, it is caused by environmental and factory-leaving factors. $Y(t)$ represents the degradation caused by degradation process and $S(t)$ represents the degradation caused by shock process. Since the shock time interval is much smaller than the total life of the electronic system, the degradation rate between each shock can be assumed as a linear function. Therefore, the degradation caused by the degradation process at time t after the n th shocks can be expressed as

$$Y(t) = \beta_1 T_1 + \beta_2 T_2 + \dots + \beta_i T_i + \beta_{i+1} \left(t - \sum_{i=1}^n T_i \right) = \sum_{i=1}^n (\beta_i T_i) + \beta_{i+1} \left(t - \sum_{i=1}^n T_i \right) \quad (2)$$

where $T_i (i = 1, 2, \dots, n)$ represents the interval between two shocks $T = [T_1, T_2, \dots, T_i, \dots, T_n]$, the arrival time of each shock follows Poisson distribution and the initial degradation rate β_1 follows normally distributed $\beta_1 \sim N(\mu_{\beta_1}, \sigma_{\beta_1}^2)$. According to the Coffin-Manson model, the degradation rate β_i can be expressed as

$$\beta_{i+1} = \eta \beta_i^\gamma = \eta \sum_{j=0}^{i-1} \gamma^j \beta_1^\gamma, \quad i = 1, 2, \dots, n \quad (3)$$

where η is the coefficient of the degradation rate that depends on the shock loads, considering the dispersion of the degradation rate, it can be assumed that η follows normally distributed $\eta \sim N(\mu_\eta, \sigma_\eta^2)$. γ is an exponential coefficient that depends on the material. The degradation caused by shock process at time t can be expressed as

$$S(t) = \sum_{i=1}^n d_i \quad (4)$$

where d_i represents the increment of each shock on the degradation process. It can be assumed to be the product of the shock load and the coefficient of transformation that can be expressed as

$$d_i = \mu w_i, \quad i = 1, 2, \dots, n \quad (5)$$

where μ is the coefficient of conversion between shock load and degradation, considering the dispersion of the degradation caused by the shock process, it can be assumed that μ follows normally distributed $\mu \sim N(\mu_\mu, \sigma_\mu^2)$. Also, the load of shocks w_i follow normally distributed $w_i \sim N(\mu_{w_i}, \sigma_{w_i}^2)$.

Assume $N(t)$ is the number of shocks arrived by the time t . When the time t is less than the time of the first shock, the degradation caused by shock process does not occur, it can be treated as the first stage of the degradation process. Therefore, the reliability of degradation process of this stage can be expressed as

$$\begin{aligned} R_S(t|N(t) = 0) &= P\{X(t) < H_0 | N(t) = 0\} \cdot P(N(t) = 0) = \\ &P\{\varphi + Y(t) < H_0 | N(t) = 0\} \cdot P(N(t) = 0) = \\ &P\{\varphi + \beta_1 t < H_0\} \cdot P(N(t) = 0). \end{aligned} \quad (6)$$

According to the above description, each shock will lead to deterioration of the material, resulting in a sudden increase in degradation and an increase in degradation rate. After the time t is greater than or equal to the time of the first shock, it enters into the second stage of the degradation process. The reliability of degradation process on the second stage can be expressed as

$$\begin{aligned} R_S(t|N(t) \geq 1) &= \sum_{i=1}^{\infty} \{P\{X(t) < H_0 | N(t) = i\} \cdot P(N(t) = i)\} = \\ &\sum_{i=1}^{\infty} \{P\{\varphi + Y(t) + S(t) < H_0 | N(t) = i\} \cdot P(N(t) = i)\} = \\ &\sum_{i=1}^{\infty} \left\{ P \left\{ \varphi + \sum_{j=1}^i (\beta_j T_j) + \beta_{i+1} \left(t - \sum_{j=1}^i T_j \right) + \sum_{j=1}^i d_j < H_0 | N(t) = i \right\} \cdot P(N(t) = i) \right\}. \end{aligned} \quad (7)$$

According to the above-mentioned description, the shock arrival time follows homogeneous Poisson process with intensity λ , so that the probability that the shocks occur for n times becomes

$$P(N(t) = n) = \frac{\exp(-\lambda t) (\lambda t)^n}{n!}, \quad n = 1, 2, \dots \quad (8)$$

According to the assumption above, φ is a constant, β_1 , η , w_i and μ are normally distributed, the probabilities of (6) and (7) are

$$\begin{aligned}
 R_S(t|N(t)=0) &= \\
 P\{\varphi + \beta_1 t < H_0 | N(t)=0\} \cdot P(N(t)=0) &= \\
 \Phi\left(\frac{H_0 - (\varphi + \mu_{\beta_1} t)}{\sigma_{\beta_1} t}\right) \cdot \exp(-\lambda t), & \quad (9) \\
 R_S(t|N(t) \geq 1) &= \sum_{i=1}^{\infty} \left\{ P\left\{ \varphi + \sum_{j=1}^i (\beta_j T_j) + \beta_{i+1} \left(t - \sum_{j=1}^i T_j \right) + \right. \right. \\
 & \quad \left. \left. \sum_{j=1}^i d_j < H_0 | N(t)=i \right\} \cdot P(N(t)=i) \right\} = \\
 & \sum_{i=1}^{\infty} \left\{ \Phi\left(\frac{H_0 - \left(\varphi + i\mu_{\beta_1} T_i + \mu_{\eta}^{i-1} \sum_{j=0}^{i-1} \mu_{\beta_1}^{j'} \left(t - \sum_{j=1}^i T_j \right) + i\mu_{\mu} \mu_{w_i} \right)}{\sqrt{\sigma_{\beta_1}^2 T_i^2 + \sigma_{\eta}^2 \sum_{j=0}^{i-1} \mu_{\beta_1}^{2j'} \left(t - \sum_{j=1}^i T_j \right) + i\sigma_{\mu}^2 \sigma_{w_i}^2}} \right) \right. \\
 & \quad \left. \frac{\exp(-\lambda t) (\lambda t)^i}{i!} \right\}. & \quad (10)
 \end{aligned}$$

3.2 Threshold descent model

In Fig. 1, lines ④ and ⑤ indicate that the hard failure threshold is determined by both the degradation process and the shock process, the hard failure threshold will be influenced by $X(t)$. Fig. 4 presents the coupled effect, where $D(t)$ is the hard failure threshold, $W(t)$ is the shock at time t . D_0 is the initial threshold, and D_i ($i = 1, 2, \dots, n$) are the thresholds at the arrival time of each shock. It is assumed that the threshold is normally distributed and the time interval is uniformly distributed.

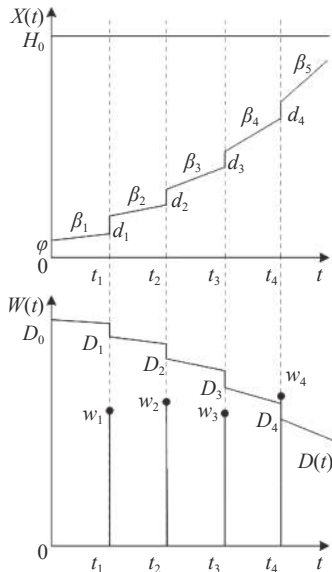


Fig. 4 Descent of hard failure threshold

According to the definition of hard failure, the electronic system fails when the shock load exceeds the hard failure threshold. There is a reciprocal transformation between the descent of hard failure threshold and the increase of degradation, assume that α is the conversion factor. The hard failure threshold can be expressed as

$$D(t) = D_0 + \alpha X(t). \quad (11)$$

The shock process can also be divided into two stages. Therefore, the reliability of shock process on the first stage can be expressed as

$$\begin{aligned}
 D(t) &= D_0 + \alpha X(t) R_H(t|N(t)=0) = \\
 P\{w_i < D_0 + \alpha X(t) | N(t)=0\} \cdot P(N(t)=0) &= \\
 P\{w_i < D_0 + \alpha(\varphi + Y(t)) | N(t)=0\} \cdot P(N(t)=0) &= \\
 P\{w_i - \alpha\varphi - \alpha\beta_1 t < D_0\} \cdot P(N(t)=0). & \quad (12)
 \end{aligned}$$

After n shocks on the electronic system at time t , the hard failure threshold can be expressed as

$$\begin{aligned}
 D(t) &= D_0 + \alpha X(t) = \\
 D_0 + \alpha\varphi + \alpha Y(t) + \alpha \sum_{i=1}^n d_i. & \quad (13)
 \end{aligned}$$

Therefore, the reliability of shock process on the second stage can be expressed as

$$\begin{aligned}
 R_H(t|N(t) \geq 1) &= \sum_{i=1}^{\infty} \{ P\{w_i < D(t) | N(t)=i\} \cdot \\
 & \quad P(N(t)=i) \} = \\
 \sum_{i=1}^{\infty} \left\{ P\left\{ w_i - \alpha\varphi - \alpha Y(t) - \alpha \sum_{j=1}^i d_j < D_0 | N(t)=i \right\} \cdot \right. \\
 & \quad \left. P(N(t)=i) \right\} = \\
 \sum_{i=1}^{\infty} \left\{ P\left\{ w_i - \alpha \sum_{j=1}^i (\beta_j T_j) - \alpha\beta_{i+1} \left(t - \sum_{j=1}^i T_j \right) - \right. \right. \\
 & \quad \left. \left. \alpha \sum_{j=1}^i d_j < D_0 + \alpha\varphi | N(t)=i \right\} \cdot P(N(t)=i) \right\}. & \quad (14)
 \end{aligned}$$

According to the assumption above, the time interval T_i of shock process follows Poisson distribution, φ is a constant, and β_1 , η , w_i and μ are normally distributed. Therefore, the probabilities of (12) and (14) are

$$\begin{aligned}
 R_H(t|N(t)=0) &= \\
 P\{w_i - \alpha\beta_1 t < D_0 + \alpha\varphi | N(t)=0\} \cdot P(N(t)=0) &= \\
 \Phi\left(\frac{D_0 + \alpha\varphi - (\mu_{w_i} - \alpha\mu_{\beta_1} t)}{\sqrt{\sigma_{w_i}^2 + \sigma_{\beta_1}^2 t^2}} \right) \cdot \exp(-\lambda t), & \quad (15)
 \end{aligned}$$

$$\begin{aligned}
 R_H(t|N(t) \geq 1) &= \\
 \sum_{i=1}^{\infty} \{ &P\{w_i < D(t)|N(t) = i\} \cdot P(N(t) = i) = \\
 \sum_{i=1}^{\infty} \left\{ P \left(w_i - \alpha\varphi - \alpha Y(t) - \alpha \sum_{j=1}^i d_j < D_0 | N(t) = i \right) \cdot \right. & \\
 P(N(t) = i) \Big\} &= \\
 \sum_{i=1}^{\infty} \left\{ P \left(w_i - \alpha \sum_{j=1}^i (\beta_j T_j) - \alpha \beta_{i+1} \left(t - \sum_{j=1}^i T_j \right) - \right. & \\
 \left. \left. \alpha \sum_{j=1}^i d_j < D_0 + \alpha\varphi | N(t) = i \right) \cdot P(N(t) = i) \right\}. & \quad (16)
 \end{aligned}$$

3.3 Modeling of system reliability

Since the shock process and the degradation process ultimately compete with each other, the electronic system reliability $R(t)$ can be expressed as follows:

$$R(t) = R_S^1(t|N(t)) \cdot R_H^1(t|N(t)) \cdot P(N(t)). \quad (17)$$

(i) When the time is less than the time of the first shock, the reliability of the electronic system can be expressed as

$$R(t|N(t) = 0) = R_S^1(t|N(t) = 0) \cdot R_H^1(t|N(t) = 0) \cdot P(N(t) = 0). \quad (18)$$

Similar to (6) and (12), (18) can be expressed as

$$\begin{aligned}
 R(t|N(t) = 0) &= \Phi \left(\frac{H_0 - (\varphi + \mu_{\beta_1} t)}{\sigma_{\beta_1} t} \right) \cdot \\
 \Phi \left(\frac{D_0 + \alpha\varphi - (\mu_{w_i} - \alpha\mu_{\beta_1} t)}{\sqrt{\sigma_{w_i}^2 + \sigma_{\beta_1}^2 t^2}} \right) \cdot \exp(-\lambda t). & \quad (19)
 \end{aligned}$$

(ii) When the time t is greater than or equal to the time of the first shock, the reliability of $N(t) \geq 1$ can be expressed as

$$R(t|N(t) \geq 1) =$$

$$\sum_{i=1}^{\infty} \{ R_S(t|N(t) = i) \cdot R_H(t|N(t) = i) \cdot P(N(t) = i) \}. \quad (20)$$

Similar to (7) and (14), (20) can be expressed as

$$\begin{aligned}
 R(t|N(t) \geq 1) &= \sum_{i=1}^{\infty} \left\{ \Phi \left(\frac{H_0 - \left(\varphi + i\mu_{\beta_1} T_i + \mu_{\eta}^{\sum_{j=0}^{i-1} \gamma^j} \mu_{\beta_1}^{\gamma^j} \left(t - \sum_{j=1}^i T_j \right) + i\mu_{\mu} \mu_{w_i} \right)}{\sqrt{\sigma_{\beta_1}^2 T_i^2 + \sigma_{\eta}^2 \sum_{j=0}^{i-1} \sigma_{\beta_1}^{2\gamma^j} \left(t - \sum_{j=1}^i T_j \right) + i\sigma_{\mu}^2 \sigma_{w_i}^2}} \right) \cdot \right. \\
 \Phi \left(\frac{D_0 + \alpha\varphi - \left(\mu_{w_i} - \alpha i\mu_{\beta_1} T_i - \alpha \mu_{\eta}^{\sum_{j=0}^{i-1} \gamma^j} \mu_{\beta_1}^{\gamma^j} \left(t - \sum_{j=1}^i T_j \right) - \alpha i\mu_{\mu} \mu_{w_i} \right)}{\sqrt{\sigma_{w_i}^2 + \sigma_{\beta_1}^2 T_i^2 + \sigma_{\eta}^2 \sum_{j=0}^{i-1} \sigma_{\beta_1}^{2\gamma^j} \left(t - \sum_{j=1}^i T_j \right) + i\sigma_{\mu}^2 \sigma_{w_i}^2}} \right) \cdot \frac{\exp(-\lambda t) (\lambda t)^i}{i!} \Big\}. & \quad (21)
 \end{aligned}$$

(iii) According to (19) and (21), the reliability of the electronic system is

$$\begin{aligned}
 R(t|N(t)) &= R(t|N(t) = 0) + R(t|N(t) \geq 1) = \Phi \left(\frac{H_0 - (\varphi + \mu_{\beta_1} t)}{\sigma_{\beta_1} t} \right) \cdot \Phi \left(\frac{D_0 + \alpha\varphi - (\mu_{w_i} - \alpha\mu_{\beta_1} t)}{\sqrt{\sigma_{w_i}^2 + \sigma_{\beta_1}^2 t^2}} \right) \cdot \\
 \exp(-\lambda t) &+ \sum_{i=1}^{\infty} \left\{ \Phi \left(\frac{H_0 - \left(\varphi + i\mu_{\beta_1} T_i + \mu_{\eta}^{\sum_{j=0}^{i-1} \gamma^j} \mu_{\beta_1}^{\gamma^j} \left(t - \sum_{j=1}^i T_j \right) + i\mu_{\mu} \mu_{w_i} \right)}{\sqrt{\sigma_{\beta_1}^2 T_i^2 + \sigma_{\eta}^2 \sum_{j=0}^{i-1} \sigma_{\beta_1}^{2\gamma^j} \left(t - \sum_{j=1}^i T_j \right) + i\sigma_{\mu}^2 \sigma_{w_i}^2}} \right) \cdot \right. \\
 \Phi \left(\frac{D_0 + \alpha\varphi - \left(\mu_{w_i} - \alpha i\mu_{\beta_1} T_i - \alpha \mu_{\eta}^{\sum_{j=0}^{i-1} \gamma^j} \mu_{\beta_1}^{\gamma^j} \left(t - \sum_{j=1}^i T_j \right) - \alpha i\mu_{\mu} \mu_{w_i} \right)}{\sqrt{\sigma_{w_i}^2 + \sigma_{\beta_1}^2 T_i^2 + \sigma_{\eta}^2 \sum_{j=0}^{i-1} \sigma_{\beta_1}^{2\gamma^j} \left(t - \sum_{j=1}^i T_j \right) + i\sigma_{\mu}^2 \sigma_{w_i}^2}} \right) \cdot \frac{\exp(-\lambda t) (\lambda t)^i}{i!} \Big\}. & \quad (22)
 \end{aligned}$$

4. Case study

4.1 Failure analysis

Electronic system operating in avionics are often affected by thermal, vibration and electromagnetic interference. Some of the wire-bonding integrated circuit chip (IC chip) devices will fail to operate due to the breaking of the bonding wire (Fig. 5).

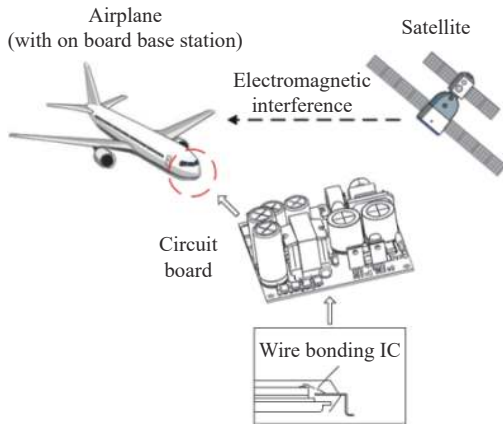


Fig. 5 Avionics in the case

The mutually DCFP effect around the wire is analyzed. Two kinds of failure mechanisms are acting on the wire. Firstly, the electric shock introduced from outside due to electromagnetic interference will lead to instantaneous wire fracture and deteriorate the local material properties. Secondly, the degradation failure mechanism of thermal fatigue will result in microcrack propagation and ultimately lead to wire fracture. The electric shock will accelerate the degradation process, and the degradation process and the shock will decrease the shock failure threshold.

4.2 Modeling parameters

The degradation process of fatigue can be predicted with (1). The required parameters for (2)–(22) are listed in Table 1. In this analysis, the initial degradation amount φ is assumed to be zero and the distributions of the values are calculated from probabilistic PoF (PPoF) method.

Table 1 Value of parameters

| Parameter | Description | Reference value | Source |
|-----------|--|-------------------------|----------------------|
| β_1 | Initial degradation rate | 3.882×10^{-10} | Design parameters |
| η | Coefficient of the degradation rate model | 5.985×10^{-10} | Zhang et al. [19] |
| γ | Index coefficient of the degradation rate model | 1.447 | Zhang et al. [19] |
| μ | Coefficient of conversion between shock load and degradation | 1.216×10^{-7} | Zhang et al. [19] |
| T_i | Time interval of each shock arrival | $\mu \sim P(6)$ | Design requirements |
| w_i/kV | Load of each shock | $w_i \sim N(3, 1.2)$ | Design requirements |
| H_0 | Degradation limit | 1 | Design parameters |
| α | Conversion factor of hard failure threshold | -6.35 | Kawauchi et al. [31] |
| D_0/kV | Initial threshold of the hard failure | 3.2 | Design parameters |

4.3 Results and discussion

4.3.1 Simulation and reliability analysis

Firstly, the mutually DCFP effect has been verified before the reliability analysis. The acceleration effect of the shock process on the degradation rate is evaluated, and the results are presented in Fig. 6, which shows the damage with and without the consideration of the acceleration effect. When the acceleration effect of the shock process on the degradation rate is not considered, the overall damage will be the dotted line in Fig. 6. The degradation process will reach the limit after 2312 d. When considering the acceleration effect, the degradation rate will increase with shocks. The damage is shown in Fig. 6 as the solid line. The degradation process will reach the limit after 2178 d. From the above conclusions, it can be seen that the acceleration effect will indeed accelerate the degradation process and make soft faults appear faster.

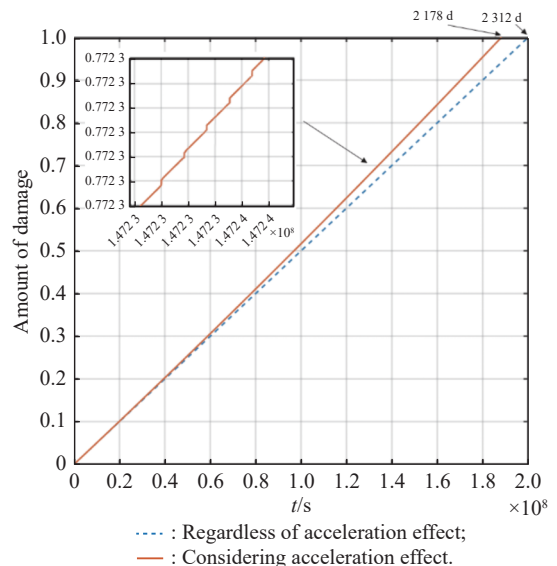


Fig. 6 Contrast of the damage

Fig. 7 presents the comparison of the hard failure threshold under different cases. When neither the influence of the degradation process nor that of the shock process is considered, the threshold remains at 8 kV. When only the decrease of the threshold caused by the shock is considered, the simulation result is the line with cross symbol. Each shock will result in the decrease of the shock threshold; therefore, the hard failure threshold will remain at the value of the previous phase, yet there will be sudden decreases at the times when a shock arrives. Thus, the overall curve is a continuous stepped curved.

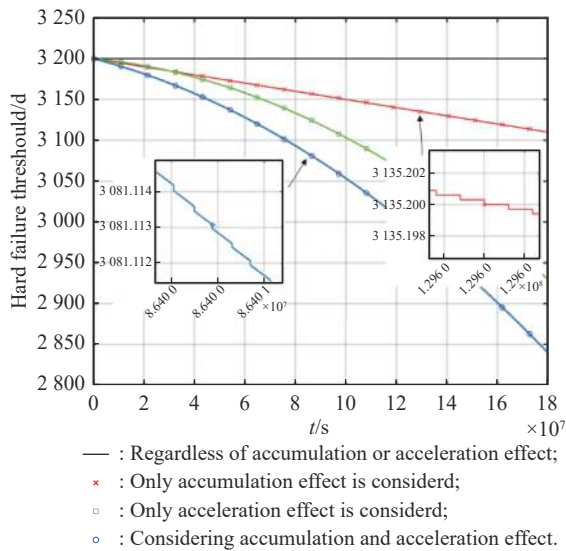


Fig. 7 Contrast of the hard failure threshold

When only the influence of degradation on the hard failure threshold is considered, the increase of the amount of degradation is proportional to the damage condition, and the hard failure threshold is shown as a smooth descend line with square symbol. The line with hollow circle in Fig. 7 is the condition when both the effect of the shock process and the effect of the degradation process on the hard failure threshold are considered. Since the two effects are assumed to be linearly accumulated, it also shown as step descent curve, however, the downward trend is more obvious. From Fig. 7, it can be seen that the cumulative effect of hard failure thresholds after considering the shock process and degradation process is significant in the evaluation of reliability.

Fig. 8 presents the comparison of the reliability with and without the consideration of mutual dependence. The line with cross symbol shows the reliability without considering any of the coupling effect, which means that the component only suffers two independent failure pro-

cesses, the shock process and the degradation process. Assuming that when the reliability decreases to 20%, the component gets to fail. The shock failure threshold and degradation rate remain constant and the failure time is 988 d. The line with square symbol is the reliability that only considers the acceleration effect. The failure time is 936 d.

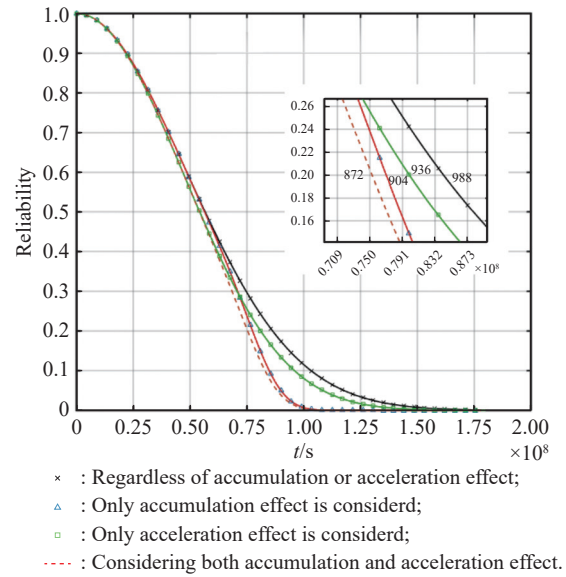


Fig. 8 Reliability of the DCFP system

The line with triangle symbol is the component reliability only considers the cumulative effect on shock threshold, the failure time is 904 d. The dotted line is the component reliability considering all the coupling effect. The voltage breakdown failure and the degradation failure compete with each other. The component ultimately fails because of hard failure, and the bonding wire breaks, the failure time is 872 d. This case is from a real aviation device, whose weak point is a wire-bonding IC. The failure data of the IC has been collected. However, the average lifetime of the IC obtained from the failure data is far lower than the prediction data provided by the manufacturer, which is carried out under the single stress conditions such as temperature and vibration without considering the DCFP effect. The lifetime obtained by the proposed method in this paper is expected to be 872 h, which is more accurate. In summary, after considering the mutually DCFP effect, the determined component reliabilities will be quite different. It is also demonstrated that the influence of the cumulative effect on the failure threshold is more serious than the influence of the acceleration effect on the degradation rate.

4.3.2 Sensitivity analysis

From (22), it can be determined that the initial degradation rate β_1 , conversion factor of hard failure threshold α , coefficient of the degradation rate model and coefficient of conversion between shock load and degradation μ are four important factors that may affect the component reliability. Because the initial degradation rate is related to the input current, its effect on the degradation rate can be neglected. The influences of β_1 , α , η and μ on component reliability are subsequently discussed as the sensitivity analysis.

Fig. 9 presents the reliability of the component with different values of α from -10.35 to -2.35 . When α is -2.35 , as the square symbol line, the failure time is 956 d. When α is -10.35 , as circle symbol line, the failure time is 796 d. A bigger absolute value of α means that degradation has more influence on shock threshold. α is related to materials strength and thermal expansion performance. Thus, selecting a material with better mechanical and thermal properties will increase component lifetime and reliability.

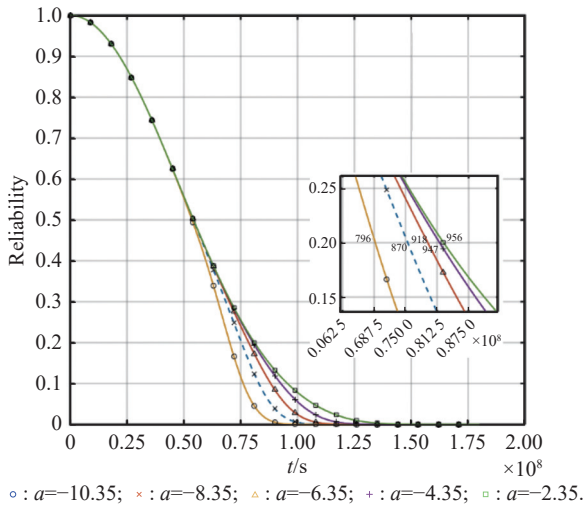


Fig. 9 Effect of α on reliability

Fig. 10 presents the reliability of the component with different values of η from 0.985×10^{-10} to 9.985×10^{-8} . When η is 0.985×10^{-10} , shown as the line with plus symbol, the failure time is 958 d. When η is 9.985×10^{-8} as the line with cross symbol, the failure time is 799 d. A larger η value indicates that the shock process has a greater influence on the shock threshold, and η is related to material properties such as toughness and stiffness.

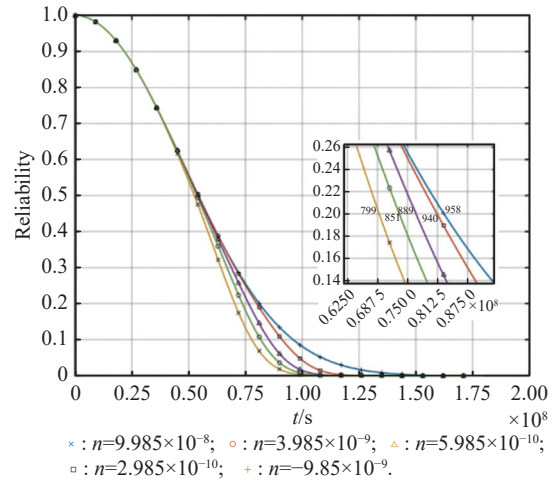


Fig. 10 Effect of η on reliability

When the voltage threshold remains constant, the distribution value of electrical shocks will have significant influence on the reliability of components. The input voltage shock is assumed to be normally distributed with an expectation of 3.2 kV, and the influence of different variances is presented in Fig. 11.

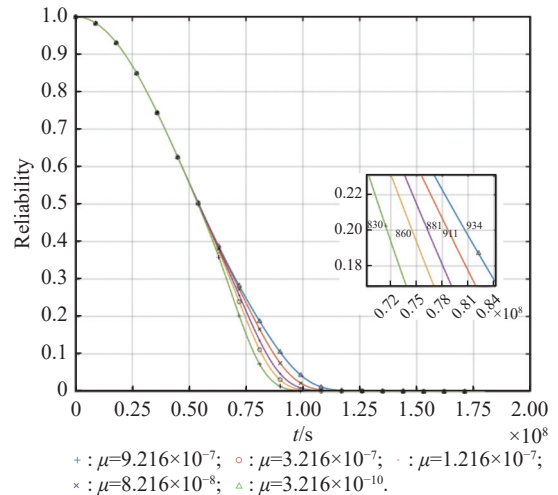


Fig. 11 Effect of μ on reliability

In Fig. 11, the value range of μ is 3.216×10^{-10} to 9.216×10^{-7} . When μ is equal to 3.216×10^{-10} as the triangle symbol line, the component failure time is 934 d. When μ is equal to 9.216×10^{-7} , the component failure time is 830 d, as the line with plus symbol in Fig. 11. In summary, the smaller the value of μ , the higher the component reliability.

The results of the case study on the avionics component demonstrate that the acceleration effect of the shock process will increase the degradation rate. In addition, the cumulative effect of the shock process and degradation process on the hard failure threshold are significant for

the evaluation of component reliability. The influence coefficient of the effect of shocks on the hard failure threshold, the influence coefficient of the effect of damage on the threshold, and the distribution of voltage shock are all sensitive factors that may affect the component reliability of wire-bonding components.

5. Conclusions

This paper presents a method to analyze the mutual dependence of competing failure processes while considering the effects of acceleration, accumulation, and competition on the degradation and the shock failure processes. The reliability of the DCFP can be theoretically obtained via the shock-degradation acceleration model and the threshold descent model.

In this paper, the reliability is calculated by the threshold decline model. This method requires the distribution of the failure time predicted by either statistical data or the PoF method. It has been demonstrated through the case that it is an effective way to evaluate reliability with the method proposed in this paper, especially when coupling effects exist in a complex electronic system. Thus, the proposed method can also be used to deal with other complex failure dependency problems. The above conclusions are verified by Monte Carlo simulation analysis.

With the increase of complexity, the simulation algorithm is expected to be optimized to solve the problems of calculation capability. Model parameters should be verified with measured data of physical products to improve accuracy. Furthermore, other types of mutual dependencies of DCFP will be studied to improve the theoretical method.

References

- [1] WANG Y, PHAM H A. Multi-objective optimization of imperfect preventive maintenance policy for dependent competing risk systems with hidden failure. *IEEE Trans. on Reliability*, 2011, 60(4): 770–781.
- [2] WANG Y, PHAM H A. Modeling the dependent competing risks with multiple degradation processes and random shock using time-varying copulas. *IEEE Trans. on Reliability*, 2012, 61(1): 13–22.
- [3] HAO S H, YANG J. Reliability analysis for dependent competing failure processes with changing degradation rate and hard failure threshold levels. *Computers & Industrial Engineering*, 2018, 118: 340–351.
- [4] KONG X F, YANG J. Reliability analysis of composite insulators subject to multiple dependent competing failure processes with shock duration and shock damage self-recovery. *Reliability Engineering and System Safety*, 2020, 204: 107166.
- [5] GAO H D, CUI L R, QIU Q G. Reliability modeling for degradation-shock dependence systems with multiple species of shocks. *Reliability Engineering and System Safety*, 2019, 185: 133–143.
- [6] SHEN J Y, ALAA E, CUI L R. Reliability analysis for multi-component systems with degradation interaction and categorized shocks. *Applied Mathematical Modelling*, 2018, 56: 487–500.
- [7] FAN M F, ZENG Z G, ZIO E, et al. A sequential Bayesian approach for remaining useful life prediction of dependent competing failure processes. *IEEE Trans. on Reliability*, 2018, 68(1): 317–329.
- [8] TANG J Y, CHEN C S, HANG L. Reliability assessment models for dependent competing failure processes considering correlations between random shocks and degradations. *Quality and Reliability Engineering International*, 2018, 35(1): 179–191.
- [9] YE Z S, TANG L C, XU H Y. A distribution-based systems reliability model under extreme shocks and natural degradation. *IEEE Trans. on Reliability*, 2011, 60(1): 246–256.
- [10] FAN M F, ZENG Z G, ZIO E, et al. Modeling dependent competing failure processes with degradation-shock dependence. *Reliability Engineering and System Safety*, 2017, 165: 422–430.
- [11] ZHU W J, FOULADIRAD M, BERENGUER C. Bicriteria maintenance policies for a system subject to competing wear and δ -shock failures. *Proceedings of the Institution of Mechanical Engineers Part O: Journal of Risk & Reliability*, 2015, 229(6): 1–16.
- [12] RAFIEE K, FENG Q M, COIT D W. Reliability analysis and condition-based maintenance for failure processes with degradation-dependent hard failure threshold. *Quality and Reliability Engineering International*, 2017, 33(7): 1351–1366.
- [13] RAFIEE K, FENG Q M, COIT D W. Reliability assessment of competing risks with generalized mixed shock models. *Reliability Engineering and System Safety*, 2017, 159: 1–11.
- [14] LIU Y, WANG Y S, FAN Z W, et al. Reliability modeling and a statistical inference method of accelerated degradation testing with multiple stresses and dependent competing failure processes. *Reliability Engineering and System Safety*, 2021, 213: 107648.
- [15] HUANG Y S, FANG C C, LU C M, et al. Optimal warranty policy for consumer electronics with dependent competing failure processes. *Reliability Engineering and System Safety*, 2022, 222: 108418.
- [16] JIANG L, FENG Q M, COIT D W. Reliability and maintenance modeling for dependent competing failure processes with shifting failure thresholds. *IEEE Trans. on Reliability*, 2012, 61(4): 932–948.
- [17] XU B, BAI G H, ZHANG Y A, et al. Failure analysis of unmanned autonomous swarm considering cascading effects. *Journal of Systems Engineering and Electronics*, 2022, 33(3): 759–770.
- [18] LI Q, ZHOU J Y, JIANG Z Q, et al. Train wheel degradation modeling and remaining useful life prediction based on mixed effect model considering dependent measurement errors. *IEEE Access*, 2019, 7: 159058–159068.
- [19] CAO Y S, LIU S F, FANG Z J, et al. Modeling ageing effects for multi-state systems with multiple components subject to competing and dependent failure processes. *Reliability Engineering and System Safety*, 2020, 199: 106890.
- [20] HAO S H, YANG J, MA X B, et al. Reliability modeling for mutually dependent competing failure processes due to degradation and random shocks. *Applied Mathematical Modelling*, 2017, 51: 232–249.
- [21] DONG W J, LIU S F, SUK B, et al. Reliability modelling for

- multi-component systems subject to stochastic deterioration and generalized cumulative shock damages. *Reliability Engineering and System Safety*, 2021, 205: 107260.
- [22] WU B, DING D. A Gamma process based model for systems subject to multiple dependent competing failure processes under Markovian environments. *Reliability Engineering and System Safety*, 2022, 217: 108112.
- [23] CHE H Y, ZENG S K, GUO J B, et al. Reliability modeling for dependent competing failure processes with mutually dependent degradation process and shock process. *Reliability Engineering and System Safety*, 2018, 180: 168–178.
- [24] ZHAO S, MAKIS V, CHEN S W, et al. Health evaluation method for degrading systems subject to dependent competing risks. *Journal of Systems Engineering and Electronics*, 2018, 29(2): 436–444.
- [25] WANG L, LI H Y, MA J. Inference for dependence competing risks from bivariate exponential model under generalized progressive hybrid censoring with partially observed failure causes. *Journal of Systems Engineering and Electronics*, 2019, 30(1): 201–208.
- [26] WANG Z Z, CHEN Y X, CAI Z Y, et al. Methods for predicting the remaining useful life of equipment in consideration of the random failure threshold. *Journal of Systems Engineering and Electronics*, 2020, 31(2): 415–431.
- [27] HUANG T T, PENG B, ZHAO Y P, et al. Reliability assessment considering stress drift and shock damage caused by stress transition shocks in a dynamic environment. *Journal of Systems Engineering and Electronics*, 2019, 30(5): 1025–1034.
- [28] CHEN Y, YANG L, YE C, et al. Failure mechanism dependence and reliability evaluation of non-repairable system. *Reliability Engineering and System Safety*, 2015, 138: 273–283.
- [29] CHEN Y, MA Q C, WANG Z, et al. Reliability analysis of k -out-of- n system with load-sharing and failure propagation effect. *Journal of Systems Engineering and Electronics*, 2021, 32(5): 1221–1231.
- [30] CHEN Y, WANG Y F, YANG S, et al. System reliability evaluation method considering physical dependency with FMT and BDD analytical algorithm. *Journal of Systems Engineering and Electronics*, 2022, 33(1): 222–232.
- [31] KAWAUCHI H, TANZAWA T. A 2V 3.8W fully-integrated clocked AC-DC charge pump with 0.5V 500 Ω vibration energy harvester. Proc. of the IEEE Asia Pacific Conference on Circuits and Systems, 2019. DOI: 10.1109/APC-CAS47518.2019.8953130.

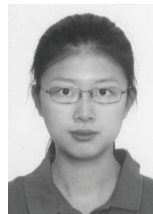
Biographies



CHEN Ying was born in 1977. She received her Ph.D. degree in instrument science and technology from Tsinghua University, Beijing, China, in 2006. She was a visiting scholar of University of California, Los Angeles during 2016–2017. She is currently an associate professor with the Science and Technology on Reliability and Environmental Engineering Laboratory, Beihang University.

Her research interests include failure behavior and reliability modeling method, and risk science.

E-mail: chenying@buaa.edu.cn



YANG Tianyu was born in 1996. She received her bachelor's degree from Beihang University in 2018. She is now a master student in the Science and Technology on Reliability and Environmental Engineering Laboratory, Beijing, China. She is specialized in the systems engineering, the reliability of electronic products and the system failure behavior.

E-mail: yangtianyu@buaa.edu.cn



WANG Yanfang was born in 1998. She received her B.S. degree from Hebei University of Technology in 2020. She is now pursuing her M.S. degree in the Science and Technology on Reliability and Environmental Engineering Laboratory, Beihang University, Beijing, China. Her primary research interests include the reliability of electronic products and the system failure behavior.

E-mail: Wang_YF@buaa.edu.cn